Electronic Supplementary Material (ESI) for Journal of Materials Chemistry A.

Supporting Information :

One-Step Solid-phase Boronation to Fabricate Self-Supported Porous FeNiB/FeNi Foam for Efficient Electrocatalytic Oxygen Evolution and Overall Water Splitting

Hefeng Yuan,[a] Shumin Wang,[a] Xundi Gu,[a] Bin Tang,[a] Jinping Li,*[b] and Xiaoguang Wang *[ab]

[a] *Laboratory of Advanced Materials and Energy Electrochemistry, Research Institute of Surface Engineering, Taiyuan University of Technology, Taiyuan, 030024, China.*

[b] *Shanxi Key Laboratory of Gas Energy Efficient and Clean Utilization, Taiyuan, Shanxi, 030024, China*

Figures:

Figure S1 (a) SEM image and (b) corresponding EDX spectrum of FeNi foam.

Figure S2 XRD pattern of FeNi foam.

Figure S3 XRD patterns of (a) FeNi@FeNiB-600, (b) FeNi@FeNiB-800 and (c) FeNi@FeNiB-900.

Figure S4 (a-c) SEM images of FeNi@FeNiB-600 at different magnifications. EDX analysis on the zones of (d) agglomerated particles and (e) smooth bottom surface of FeNi@FeNiB-600. Inset: corresponding SEM images.

Figure S5 (a,d) SEM images on different area of FeNi@FeNiB-800. (b,c) high-magnification SEM images of different area from (a). (e,f) High-magnification SEM images of different area from (d). (g,h) EDX analysis on different area of FeNi@FeNiB-800. Inset: corresponding SEM images.

Figure S6 (a-c) SEM images of FeNi@FeNiB-900 at different magnifications. (d,e) EDX analysis on different area of FeNi@FeNiB-900. Inset: corresponding SEM images.

Figure S7 Cross-section SEM images of (a) FeNi@FeNiB-600, (b) FeNi@FeNiB-700, (c) FeNi@FeNiB-800 and (d) FeNi@FeNiB-900.

Figure S8 XPS survey profiles for as-prepared FeNi@FeNiB-700.

Figure S9 Overpotential at 10 mA cm^{-2} and Tafel slope of state-of-the-art noble-metal-free OER electrocatalysts in 1.0 M KOH from Table S1.

Figure S10 Cyclic voltammogram in the double layer region at the scan rate of 5, 10, 20, 40, 60, 80 and 100 mV s^{-1} of (a) FeNi foam, (b) FeNi@FeNiB-600, (c) FeNi@FeNiB-700, (d) FeNi@FeNiB-800 and (e) FeNi@FeNiB-900.

Figure S11 Nyquist plots of FeNi foam, FeNi@FeNiB-600, FeNi@FeNiB-700, FeNi@FeNiB-800 and FeNi@FeNiB-900 in 1.0 M KOH under the potentials of (a) 1.23 V (vs. RHE) and (b) 1.40 V (vs. RHE), respectively.

Figure S12 Equivalent circuit used for fitting the Nyquist plots.

Figure S13 (a) Cyclic voltammograms of FeNi@FeNiB-700 at different scan rates increasing from 5 mV s^{-1} to 30 mV s^{-1} in 1.0 M KOH. (b) Corresponding plots of

oxidation peak current versus scan rate on FeNi@FeNiB-700.

Figure S14. The digital images of electrolyte (a) before and (b) after long-term OER characterization.

Figure S15 The amount of gas theoretically calculated and experimentally measured versus time for FeNi@FeNiB-700.

Figure S16 (a) Comparison of XRD spectra of original FeNi@FeNiB-700 and post-tested FeNi@FeNiB-700 with chronopotentiometric (CP) test for 12 h. (b) Detailed XRD pattern of FeNi@FeNiB-700-CP.

Figure S17 XPS survey profiles for FeNi@FeNiB-700 after OER stability test.

Figure S18 High resolution XPS spectra of the (a) Fe 2p, (b) Ni 2p, (c) B 1s and (d) O 1s for FeNi@FeNiB-700 after long-term stability test.

Figure S19 DFT calculations: (a-c) are the models of Ni_2B, Ni_4B_3 and Fe-Ni_4B_3; (d-f) are the models of O-adsorbed Ni_2B, Ni_4B_3 and Fe-Ni_4B_3. (Blue: Ni, purple: Fe, pink: B, red: O)

Figure S20 Polarization curves of FeNi@FeNiB-700, FeNi foam, CoNi foam, Ni foam, FeNi-P foam, CoNi-P foam, Ni-P foam and Pt/C toward the HER in 1.0 M KOH solution.

Tables:

Table S1 Comparison of Tafel slope and required overpotential at 10 mA cm^{-2} (η_{10}) for FeNi@FeNiB-700 with many of reported state-of-the-art noble metal free OER electrocatalysts in alkaline media.

Table S2 EIS parameters (R_s and R_{ct}) of FeNi@FeNiB-X (X=600,700,800,900) at controlled-potentials of 1.23 V, 1.40 V and 1.50 V vs. RHE, respectively.

Table S3 Quantitative analysis of original FeNi@FeNiB-700 and post-tested FeNi@FeNiB-700 for 12 h from XPS measurements.

DFT calculations

Based on the first-principle calculation, all theoretical calculations were performed on the plane-wave software code VASP (Vienna Ab Initio Simulation Package).[1-3] The projector augmented wave (PAW) model with the Perdew–Burke–Ernzerhof (PBE) generalized gradient approximation (GGA) exchange–correlation functional was employed to describe the interactions between core and electrons.[4] The convergence threshold for structural optimization was set as 10^{-5} eV in energy and -0.05 eV in force. Considering the plane-wave basis restriction, the cutoff energy was set as 450 eV. Meanwhile, the Brillouin zone was sampled with the Monkhorst−Pack scheme. Monkhorst−Pack k-point setups were 3 × 3 × 3 and 3 × 3 × 1 for bulk and slab geometry optimization, respectively.

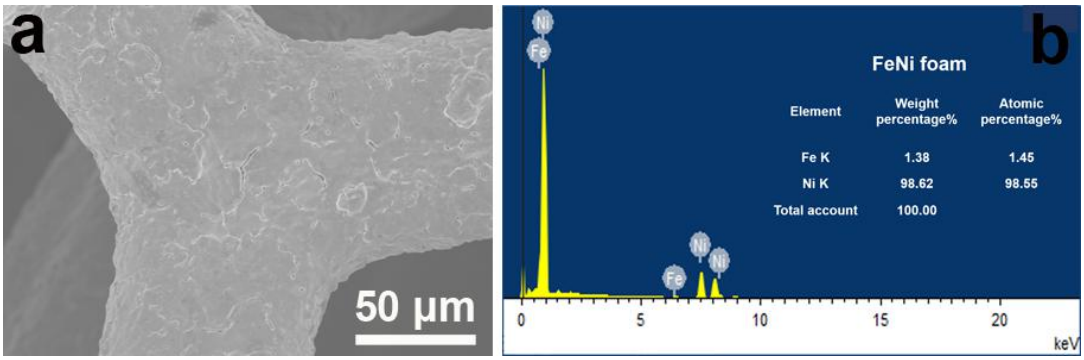

Figure S1. (a) SEM image and (b) corresponding EDX spectrum of FeNi foam.

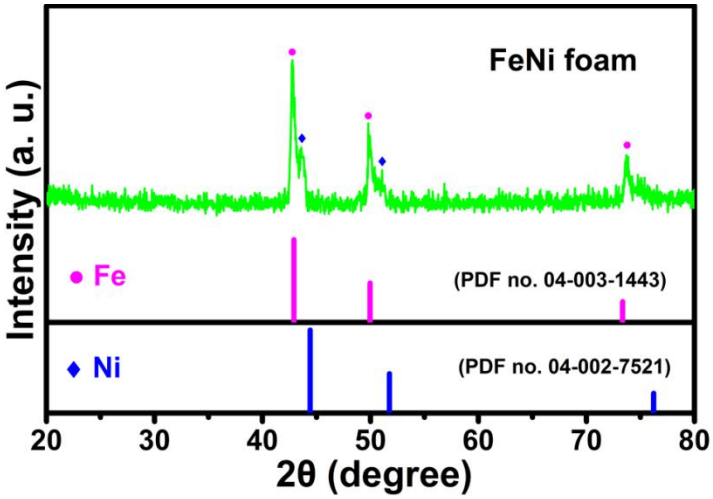

Figure S2. XRD pattern of FeNi foam.

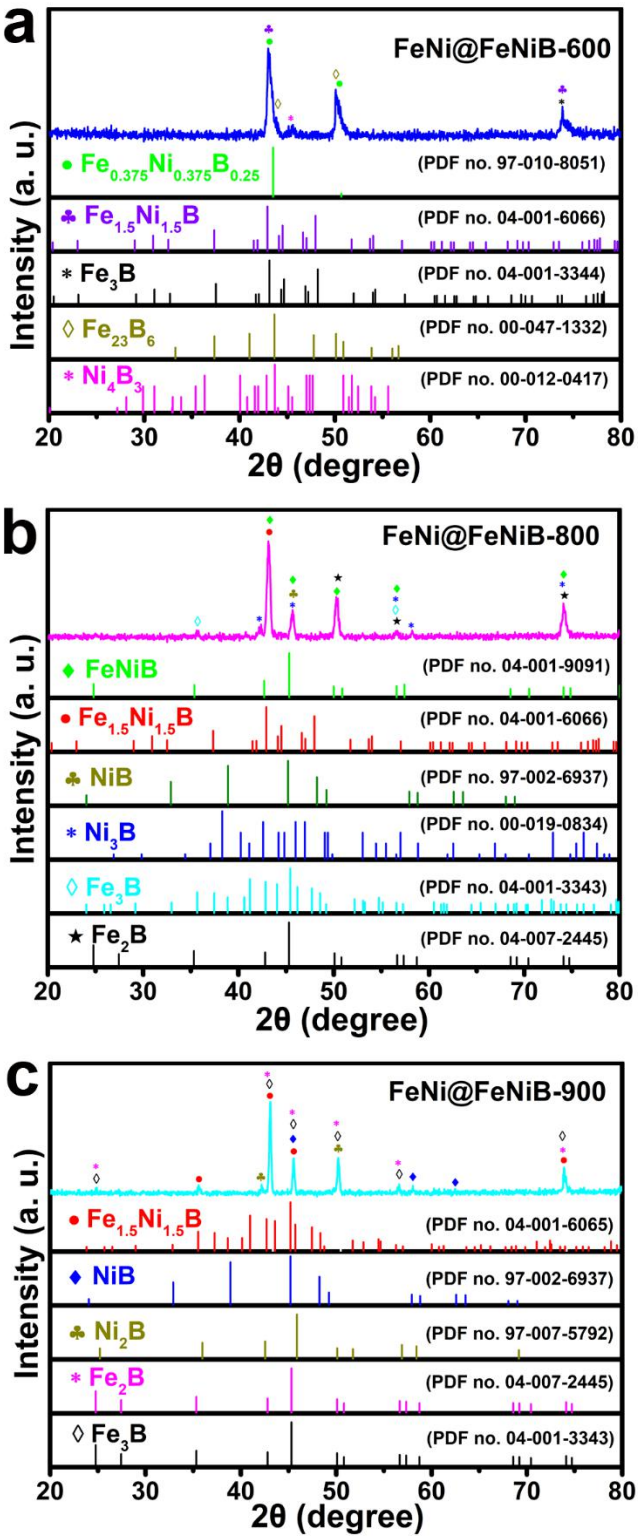

Figure S3. XRD patterns of (a) FeNi@FeNiB-600, (b) FeNi@FeNiB-800 and (c) FeNi@FeNiB-900.

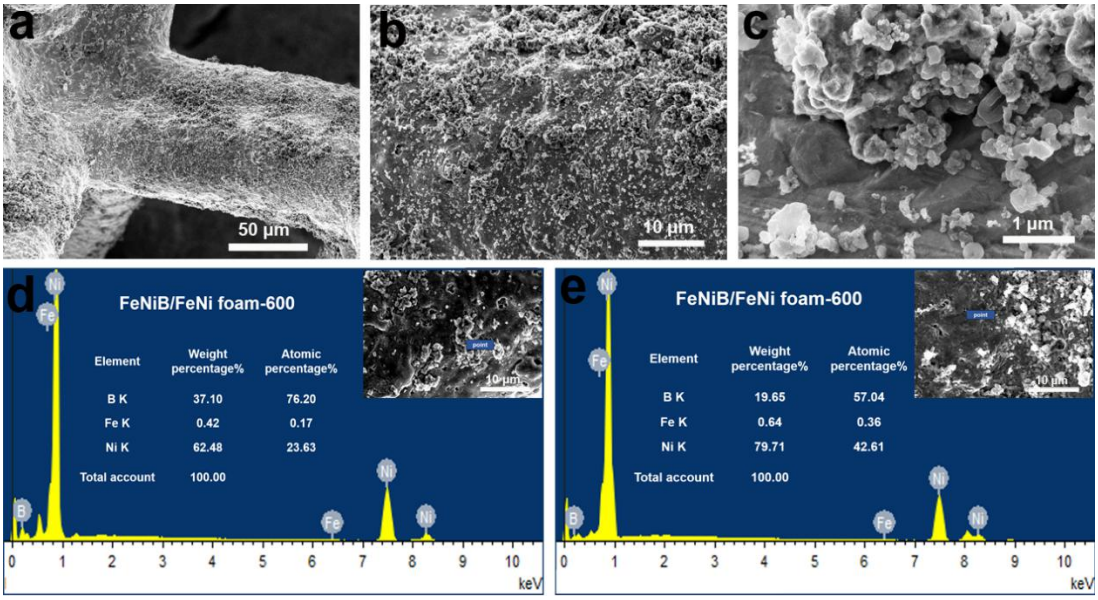

Figure S4. (a-c) SEM images of FeNi@FeNiB-600 at different magnifications. EDX analysis on the zones of (d) agglomerated particles and (e) smooth bottom surface of FeNi@FeNiB-600. Inset: corresponding SEM images.

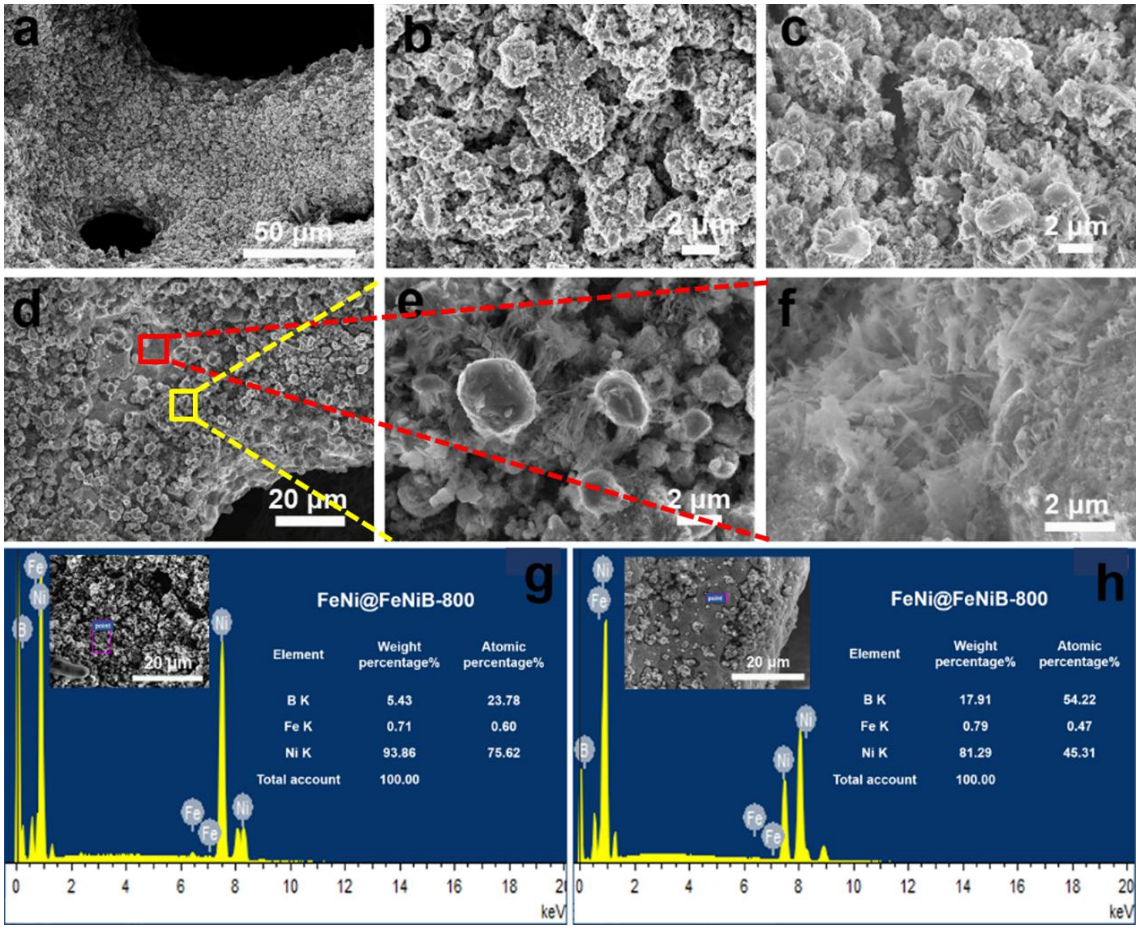

Figure S5. (a,d) SEM images on different area of FeNi@FeNiB-800. (b,c) high-magnification SEM images of different area from (a). (e,f) High-magnification SEM images of different area from (d). (g,h) EDX analysis on different area of FeNi@FeNiB-800. Inset: corresponding SEM images.

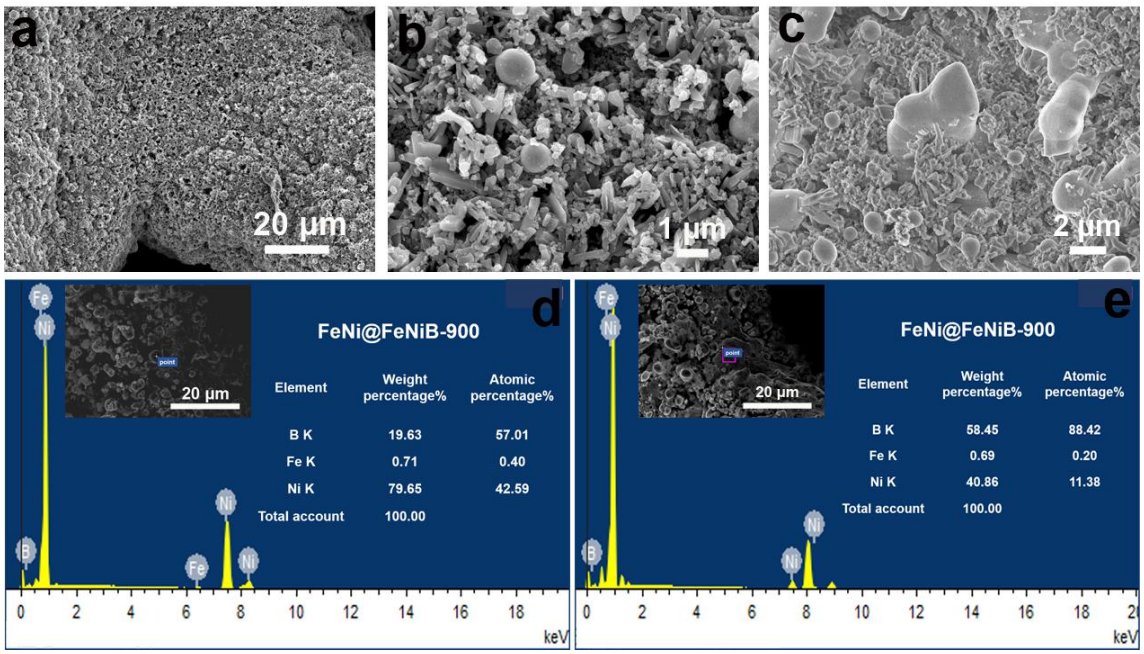

Figure S6. (a-c) SEM images of FeNi@FeNiB-900 at different magnifications. (d,e) EDX analysis on different area of FeNi@FeNiB-900. Inset: corresponding SEM images.

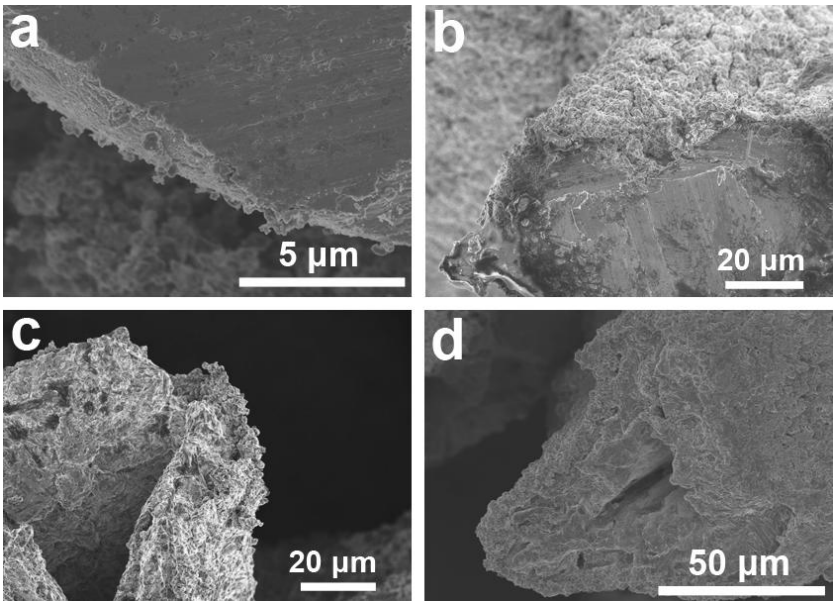

Figure S7. Cross-section SEM images of (a) FeNi@FeNiB-600, (b) FeNi@FeNiB-700, (c) FeNi@FeNiB-800 and (d) FeNi@FeNiB-900.

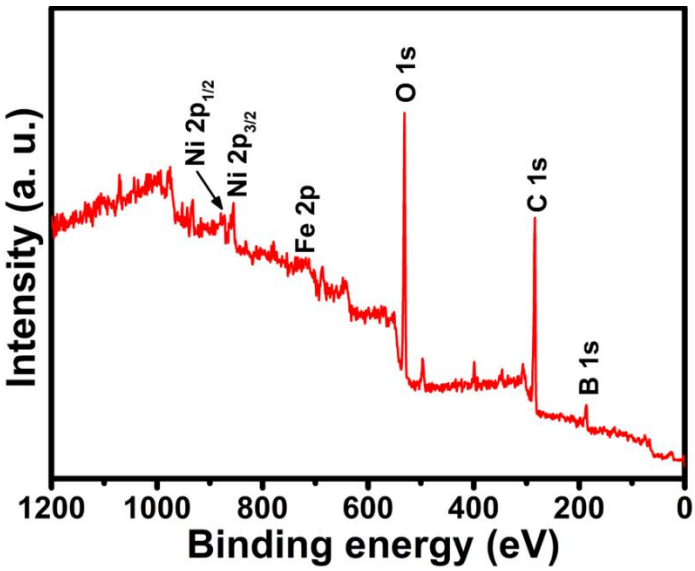

Figure S8. XPS survey profiles for as-prepared FeNi@FeNiB-700.

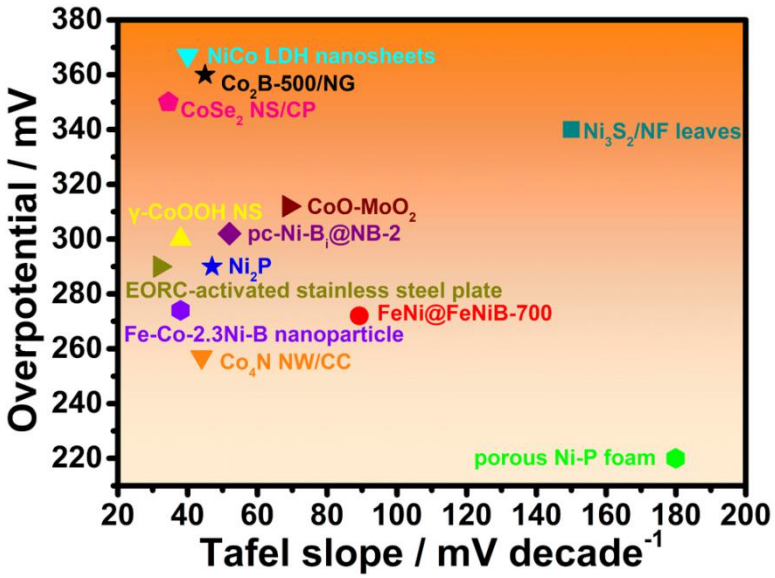

Figure S9. Overpotential at 10 mA cm^{-2} and Tafel slope of state-of-the-art noble-metal-free OER electrocatalysts in 1.0 M KOH from Table S1.

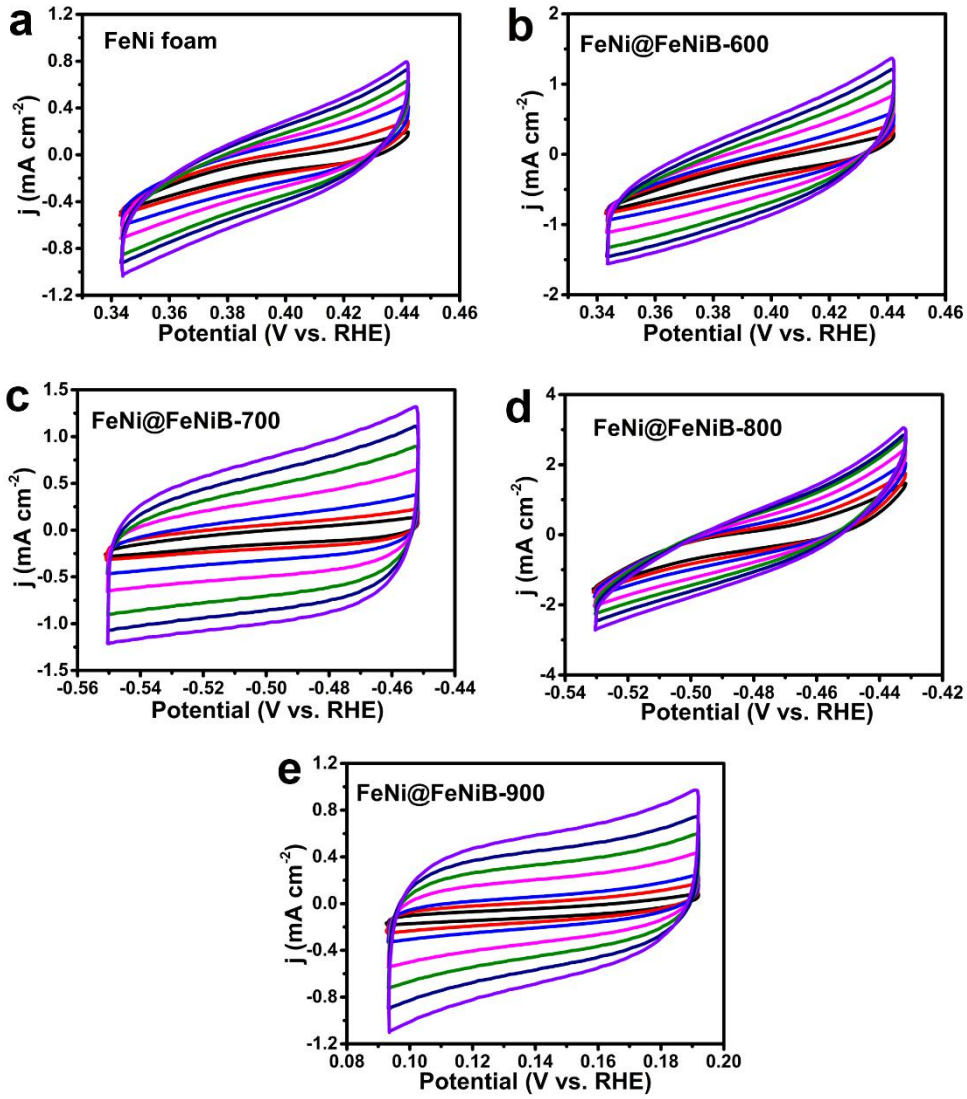

Figure S10. Cyclic voltammogram in the double layer region at the scan rate of 5, 10, 20, 40, 60, 80 and 100 mV s^{-1} of (a) FeNi foam, (b) FeNi@FeNiB-600, (c) FeNi@FeNiB-700, (d) FeNi@FeNiB-800 and (e) FeNi@FeNiB-900.

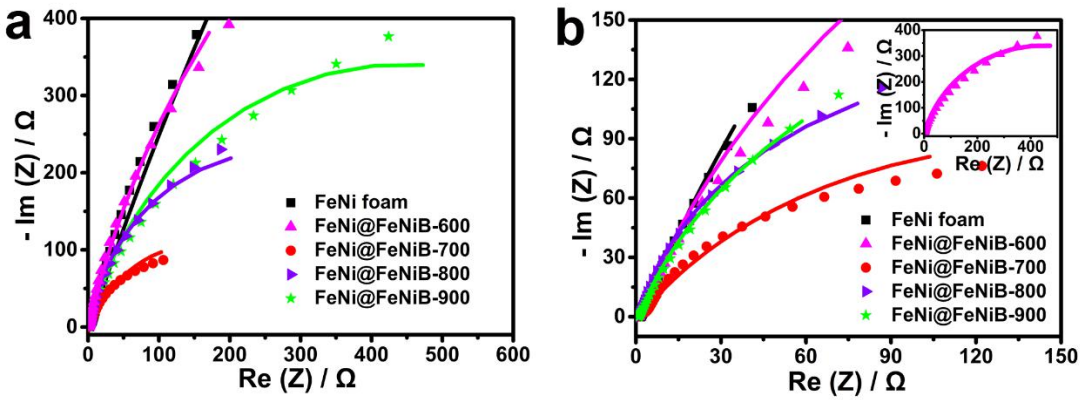

Figure S11. Nyquist plots of FeNi foam, FeNi@FeNiB-600, FeNi@FeNiB-700, FeNi@FeNiB-800 and FeNi@FeNiB-900 in 1.0 M KOH under the potentials of (a) 1.23 V (vs RHE) and (b) 1.40 V (vs RHE), respectively.

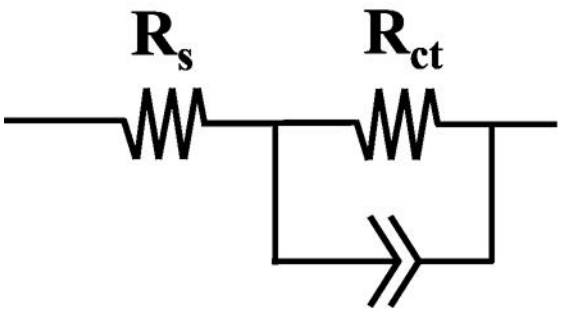

Figure S12. Equivalent circuit used for fitting the Nyquist plots.

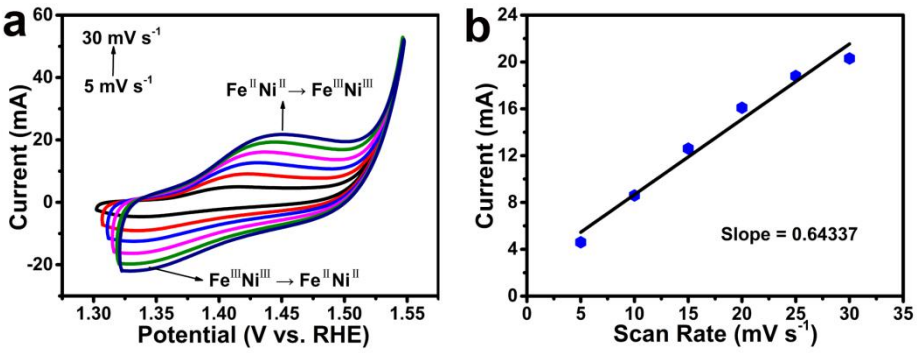

Figure S13. (a) Cyclic voltammograms of FeNi@FeNiB-700 at different scan rates increasing from 5 mV s^{-1} to 30 mV s^{-1} in 1.0 M KOH. (b) Corresponding plots of oxidation peak current versus scan rate on FeNi@FeNiB-700.

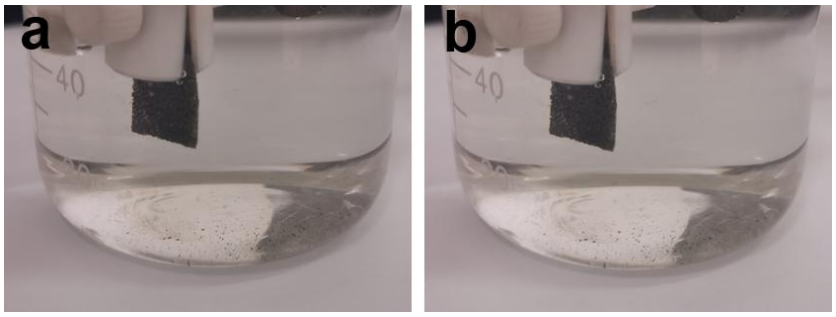

Figure S14. The digital images of electrolyte (a) before and (b) after long-term OER characterization.

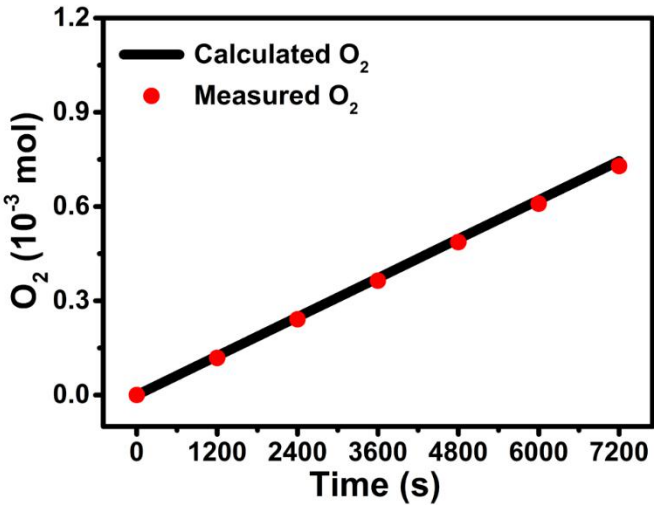

Figure S15. The amount of gas theoretically calculated and experimentally measured versus time for FeNi@FeNiB-700.

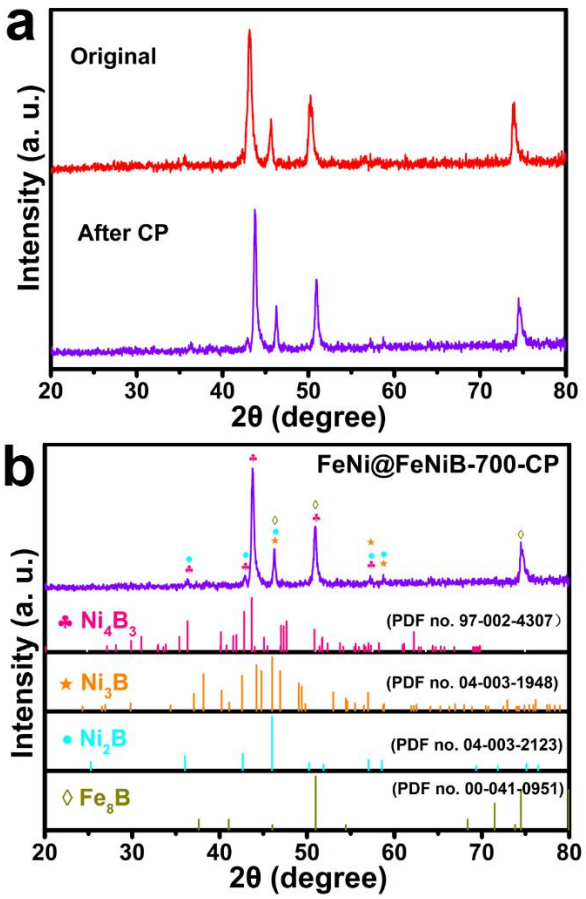

Figure S16. (a) Comparison of XRD spectra of original FeNi@FeNiB-700 and post-tested FeNi@FeNiB-700 with chronopotentiometric (CP) test for 12 h. (b) Detailed XRD pattern of FeNi@FeNiB-700-CP.

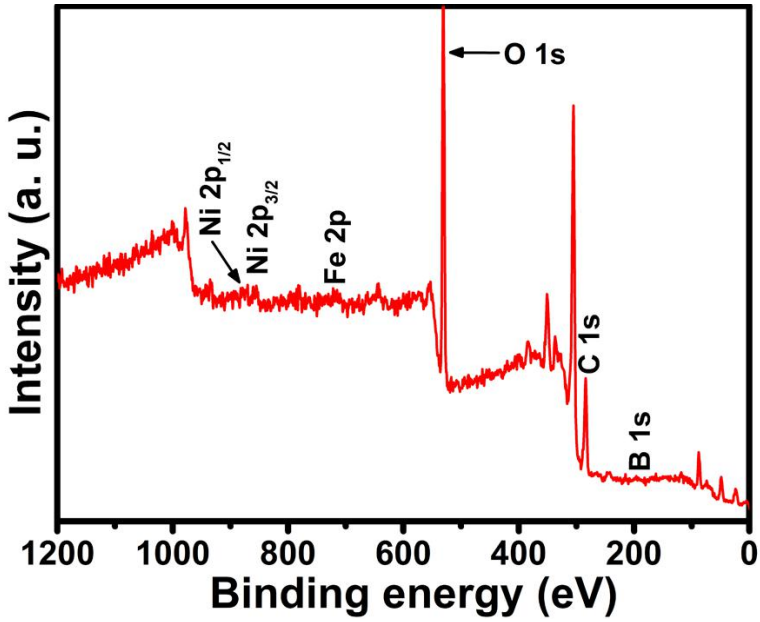

Figure S17. XPS survey profiles for FeNi@FeNiB-700 after OER stability test.

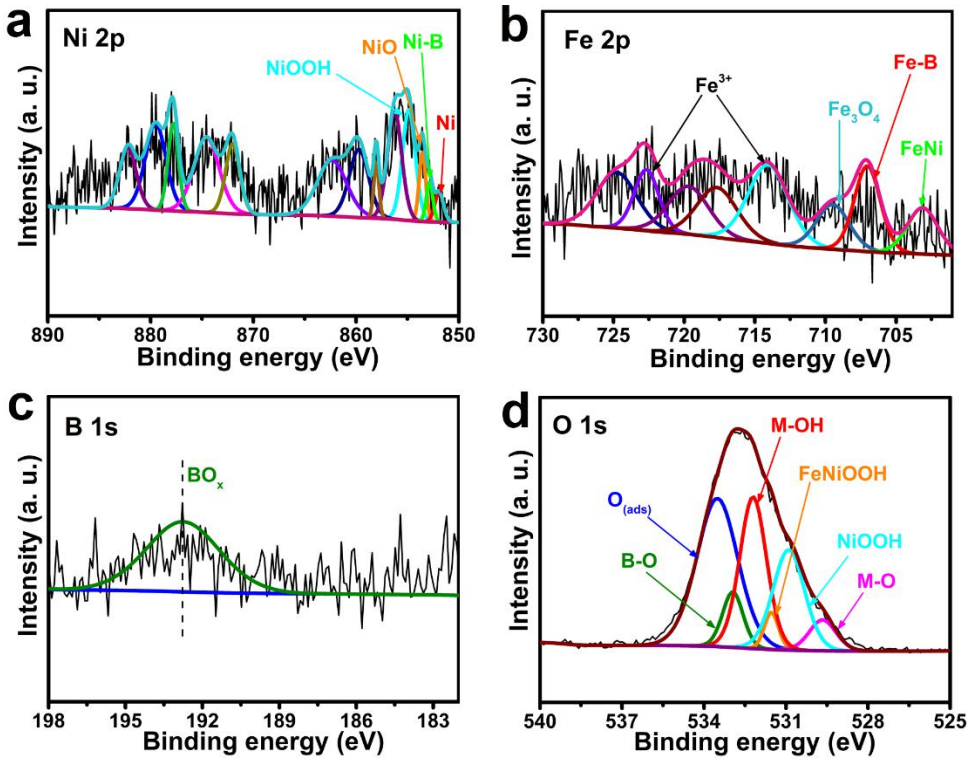

Figure S18. High resolution XPS spectra of the (a) Fe 2p, (b) Ni 2p, (c) B 1s and (d) O 1s for FeNi@FeNiB-700 after long-term stability test.

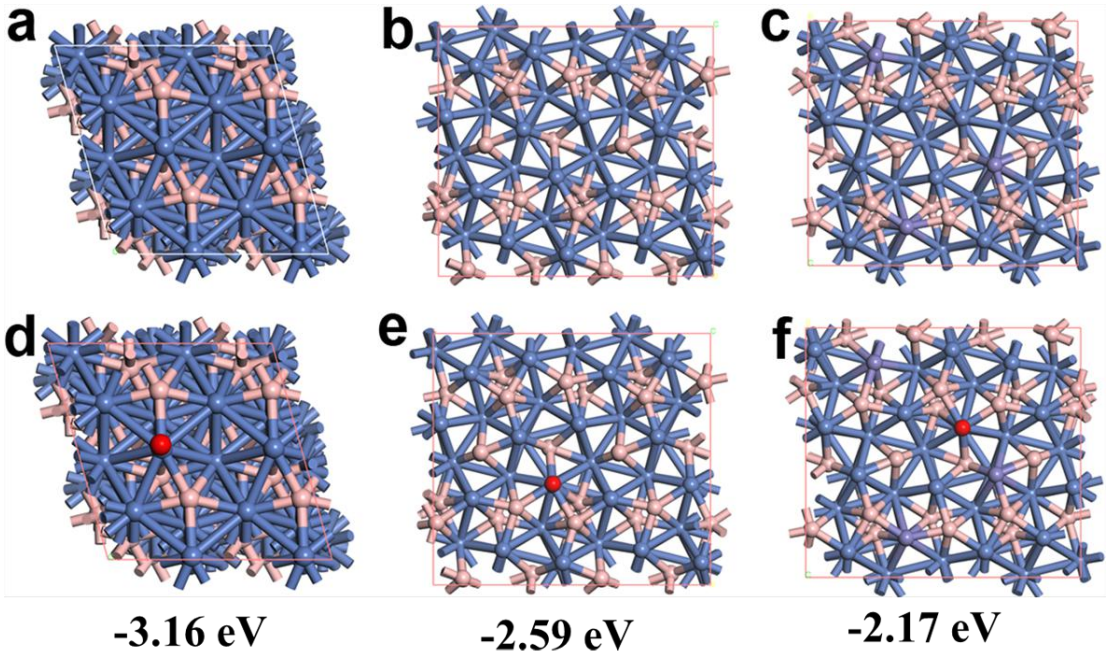

Figure S19. DFT calculations: (a-c) are the models of Ni_2B, Ni_4B_3 and Fe-Ni_4B_3; (d-f) are the models of O-adsorbed Ni_2B, Ni_4B_3 and Fe-Ni_4B_3. (Blue: Ni, purple: Fe, pink: B, red: O)

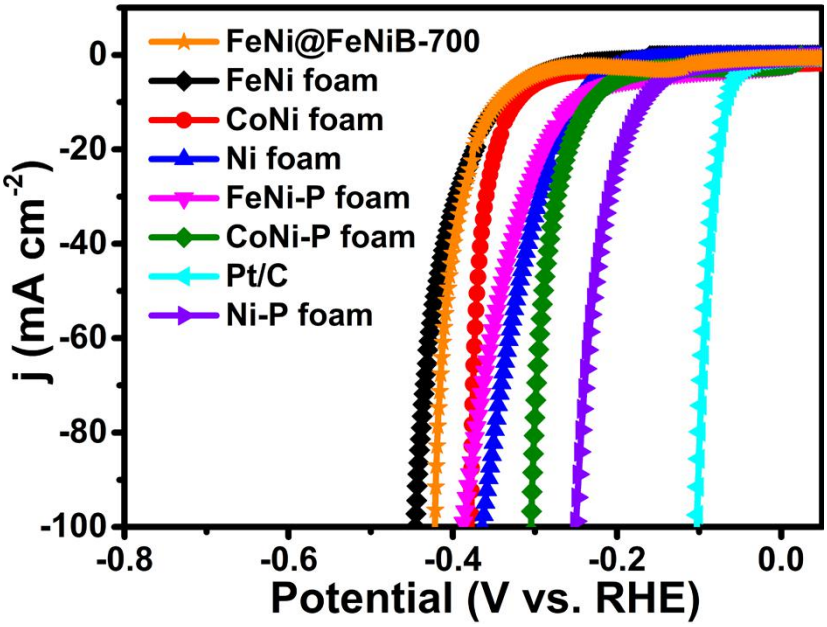

Figure S20. Polarization curves of FeNi@FeNiB-700, FeNi foam, CoNi foam, Ni foam, FeNi-P foam, CoNi-P foam, Ni-P foam and Pt/C toward the HER in 1.0 M KOH solution.

Table S1 Comparison of Tafel slope and required overpotential at 10 mA cm^{-2} (η_{10}) for FeNi@FeNiB-700 with many of reported state-of-the-art noble-metal-free OER electrocatalysts in alkaline media.

Catalysts	η_{10} (mV)	Tafel slope (mV dec^{-1})	Reference
FeNiB/FeNi foam-700	272	89.2	This work
porous Ni–P foam	220	179.9	[5]
Ni_2P	290	47	[6]
NiCo LDH nanosheets	367	40	[7]
pc-Ni-B_i@NB-2	302	52	[8]
Co_2B-500/NG	360	45	[9]
Fe–Co–2.3Ni–B nanoparticle	274	38	[10]
γ-CoOOH NS	300	38	[11]
Co_4N NW/CC	257	44	[12]
Ni_3S_2/NF leaves	340	150	[13]
$CoSe_2$ NS@CP	350	34.5	[14]
CoO–MoO_2	312	69	[15]
EORC-activated stainless steel plate	290	32	[16]

Table S2 EIS parameters (R_s and R_{ct}) of FeNi@FeNiB-X (X=600,700,800,900) at controlled-potentials of 1.23 V, 1.40 V and 1.50 V vs. RHE, respectively.

sample	1.23 V		1.40 V		1.50 V	
	$R_s(\Omega)$	$R_{ct}(\Omega)$	$R_s(\Omega)$	$R_{ct}(\Omega)$	$R_s(\Omega)$	$R_{ct}(\Omega)$
FeNi foam	2	8910	1.832	1971	2.875	648.9
FeNi@FeNiB-600	0.787	2334	0.754	335.7	0.838	38.5
FeNi@FeNiB-700	0.846	328.79	1.059	35.03	0.493	25.16
FeNi@FeNiB-800	1.296	534.6	0.981	299.4	1.875	36.16
FeNi@FeNiB-900	1.705	1061	1.066	415.4	2.232	111.6

Table S3 Quantitative analysis of original FeNi@FeNiB-700 and post-tested FeNi@FeNiB-700 for 12 h from XPS measurements.

	Ni (at. %)	Fe (at. %)	B (at. %)	O (at. %)
Before OER	5.24	2.26	31.81	60.69
After OER	3.15	2.43	3.40	91.01

Reference

[1] G. Kresse, J. Furthmüller, *Phys. Rev. B* **1996,** *54,* 11169.

[2] H. J. Meng, W. J. Zhang, Z. Z. Ma, F. Zhang, B. Tang, J. P. Li, X. G. Wang, *ACS Appl. Mater. Interfaces* **2018,** *10,* 2430−2441.

[3] W. J. Zhang, J. Zheng, X. D. Gu, B. Tang, J. P. Li, X. G. Wang, *Nanoscale* **2019,** *11,* 9353-9361.

[4] J. P. Perdew, K. Burke, M. Ernzerhof, *Phys. Rev. Lett.* **1996,** *77,* 3865-3868.

[5]X. G. Wang, W. Li, D. H. Xiong, L. F. Liu, *J. Mater. Chem. A* **2016,** *4,* 5639–5646.

[6] E. J. Popczun, J. R. McKone, C. G. Read, A. J. Biacchi, A. M. Wiltrout, N. S. Lewis, R. E. Schaak, *J. Am. Chem. Soc.* **2013,** *135,* 9267-9270.

[7] H. F. Liang, F. Meng, M. Caban-Acevedo, L. Li, A. Forticaux, L. Xiu, Z. C. Wang, S. Jin, *Nano Lett.* **2015,** *15*, 1421-1427.

[8] W. J. Jiang, S. Niu, T. Tang, Q. H. Zhang, X. Z. Liu, Y. Zhang, Y. Y. Chen, J. H. Li, L. Gu, L. J. Wan, J. S. Hu, *Angew. Chem. Int. Ed.* **2017,** *56*, 6572-6577.

[9] J. Masa, P. Weide, D. Peeters, I. Sinev, W. Xia, Z. Y. Sun, C. Somsen, M. Muhler, W. Schuhmann, *Adv. Energy Mater.* **2016,** *6*, 1502313.

[10] J. M. V. Nsanzimana, Y. Peng, Y. Y. Xu, L. Thia, C. Wang, B. Y. Xia, X. Wang, *Adv. Energy Mater.* **2018,** *8*, 1701475.

[11] H. T. Wang, H. W. Lee, Y. Deng, Z. Y. Lu, P. C. Hsu, Y. Y. Liu, D. C. Lin, Y. Cui, *Nat. Commun.* **2015,** *6*, 7261.

[12] P. Z. Chen, K. Xu, Z. W. Fang, Y. Tong, J. C. Wu, X. L. Lu, X. Peng, H. Ding, C. Z. Wu, Y. Xie, *Angew. Chem.* **2015,** *54*, 14710-14714.

[13] T. Zhu, L. L. Zhu, J. Wang, G. W. Ho, *J. Mater. Chem. A* **2016,** 4, 13916.

[14] Y. Zhou, H. Q. Xiao, S. Zhang, Y. P. Li, S. T. Wang, Z. J. Wang, C. H. An, J. Zhang, *Electrochim. Acta* **2017,** *241,* 106-115.

[15] F. L. Lyu, Y. C. Bai, Z. W. Li, W. J. Xu, Q. F. Wang, J. Mao, L. Wang, X. W. Zhang, Y. D. Yin, *Adv. Funct. Mater.* **2017,** *27*, 1702324.

[16] H. X. Zhong, J. Wang, F. L. Meng, X. B. Zhang, *Angew. Chem. Int. Ed.* **2016,** *55,* 9937-9941.